



Geophysical Research Letters*



RESEARCH LETTER

10.1029/2023GL104910

Key Points:

- The March 2022 Antarctic heatwave registered the warmest temperature anomaly on record, and resulted from extreme atmospheric heat fluxes
- A widely used climate model cannot simulate equivalent events in a large ensemble, a bias that is improved after nudging its winds to observations
- The thermodynamic amplification of the heatwave by climate change was 2°C, and equivalent heatwaves may warm a further 5–6°C by 2100

Supporting Information:

Supporting Information may be found in the online version of this article.

Correspondence to:

E. Blanchard-Wrigglesworth, edwardbw@uw.edu

Citation:

Blanchard-Wrigglesworth, E., Cox, T., Espinosa, Z. I., & Donohoe, A. (2023). The largest ever recorded heatwave—Characteristics and attribution of the Antarctic heatwave of March 2022. *Geophysical Research Letters*, 50, e2023GL104910. https://doi.org/10.1029/2023GL104910

Received 9 JUN 2023 Accepted 3 AUG 2023

© 2023. The Authors.
This is an open access article under
the terms of the Creative Commons
Attribution-NonCommercial-NoDerivs
License, which permits use and
distribution in any medium, provided the
original work is properly cited, the use is
non-commercial and no modifications or
adaptations are made.

The Largest Ever Recorded Heatwave—Characteristics and Attribution of the Antarctic Heatwave of March 2022

Edward Blanchard-Wrigglesworth¹, Tyler Cox¹, Zachary I. Espinosa¹, and Aaron Donohoe^{1,2}

¹Department of Atmospheric Sciences, University of Washington, Seattle, WA, USA, ²Applied Physics Lab, University of Washington, Seattle, WA, USA

Abstract An unprecedented heatwave impacted East Antarctica in March 2022, peaking at 39°C above climatology, the largest temperature anomaly ever recorded globally. We investigate the causes of the heatwave, the impact of climate change, and a climate model's ability in simulating such an event. The heatwave, which was skillfully forecast, resulted from a highly anomalous large-scale circulation pattern that advected an Australian airmass to East Antarctica in 4 days and produced record atmospheric heat fluxes. Southern Ocean sea surface temperatures anomalies had a minimal impact on the heatwave's amplitude. Simulations from a climate model fail to simulate such a large temperature anomaly mostly due to biases in its large-scale circulation variability, showcasing a pathway for future model improvement in simulating extreme heatwaves. The heatwave was made 2°C warmer by climate change, and end of 21st century heatwaves may be an additional 5–6°C warmer, raising the prospect of near-melting temperatures over the interior of East Antarctica.

Plain Language Summary An extreme heatwave took place in East Antarctica in March 2022, which registered the most anomalous temperatures above local climatology ever recorded. The heatwave resulted from a highly unusual weather pattern which produced strong northerly winds and imported warm and moist air from Australia. Weather forecast models skillfully predicted the heatwave up to 8 days in advance. While the heatwave took place soon after the record sea ice minimum of February, Southern Ocean sea surface temperature anomalies had a minimal impact on the magnitude of the heatwave. We have found that a widely used climate model cannot simulate heatwaves of this magnitude, but when the model's winds in the free atmosphere are nudged toward observations, the model can simulate a heatwave closer to observations, suggesting model improvements in atmospheric circulation variability would lead to better heatwave simulation. To address the impact of climate change, we have re-run the model simulations, nudging to the same winds but under past and future anthropogenic forcing. We find that the heatwave was made 2°C warmer by climate change, and future end of century heatwaves to be 5–6°C warmer, suggesting the possibility of near-melting temperatures over the East Antarctic ice cap during extreme heatwaves.

1. Introduction

Extreme events have an oversized footprint on socioeconomic impacts and serve as litmus tests for environmental system models. Understanding their physical causes, predictability, and how their frequency and amplitude may be impacted by climate change is of crucial importance (Stott et al., 2016). Heatwaves are among the most impactful extreme weather events (e.g., Konovalov et al., 2011; Lesk et al., 2016; Sutanto et al., 2020; White et al., 2023), and their frequency and intensity are already increasing as the climate warms (e.g., Perkins-Kirkpatrick & Lewis, 2020). Heatwaves in polar regions are coming under increased scrutiny (e.g., González-Herrero et al., 2022; Robinson et al., 2020; Turner et al., 2022b), motivated by their increased frequency (Dobricic et al., 2020), the importance of polar regions to global climate (e.g., England et al., 2020) and sea level (e.g., DeConto & Pollard, 2016), and impact of warming on surface melting (e.g., Tedesco & Fettweis, 2020; Trusel et al., 2015).

In March 2022, an extreme heatwave took place over eastern East Antarctica (EEA) associated with a large-scale atmospheric ridging event (Wang et al., 2022). Interestingly, it followed the lowest Antarctic sea ice extent on record up to that time (Turner et al., 2022a), observed in February 2022. Here we describe the heatwave and its causes, and investigate the forecast skill of weather forecasts in predicting the heatwave. We also use a global climate model (GCM) to ask how well can it simulate an equivalent event, to assess the impact of global warming

2. Methods and Data

2.1. Heatwave Analysis

To characterize the heatwave, we use hourly weather station data over 1996–2022 and 12 UTC radiosondes over 2006–2022 from the Dome C station in East Antarctica (75°S, 123°E, and 3,250 m above sea level), and ERA5 reanalysis data (Hersbach et al., 2020). We also use temperature observations from the Dome C tower at 2 and 40 m heights, and NOAA's HYSPLIT back trajectories (Stein et al., 2015). To rank the East Antarctic March 2022 heatwave globally, we use global weather station data from the Global Historical Climatology Network using each station's full record, and ERA5 over 1979–2022 (see further details in Supporting Information S1). We use the NSIDC sea ice concentration (SIC) climate data record product version 4 (Meier et al., 2021) and the NOAA ERSSTv5 SST product (Huang et al., 2017).

2.2. Atmospheric Fluxes

To calculate the atmospheric heat flux (AHT) convergence over EEA, we vertically integrate the product of winds and moist-static energy (MSE) in the ERA5 reanalysis at each six hourly time step. The MSE is defined as the sum of the sensible, latent, and potential energy:

$$MSE = c_p T + L_v Q + gZ, (1)$$

where c_p is the specific heat of air, T is temperature, L_v is the latent heat of vaporization of water, Q is the specific humidity, g is the gravitational acceleration, and Z is geopotential height. The AHT convergence is then defined using the advective form of the flux equations (Donohoe & Battisti, 2013):

$$-\nabla \cdot AHT = \int_0^{\overline{Ps}} -(U, V) * \nabla MSE - MSE^{\dagger} * \nabla \cdot (U, V) dp$$
 (2)

where daggers (†) represent the anomaly from the vertical average and \overline{Ps} is the time mean surface pressure while all other variables are instantaneous values. The first term on the right-hand side represents the lateral advection of MSE. The second term represents the vertical advection diagnosed from Boussinesq continuity equation, with low level convergence (where MSE† < 0 in a stable atmosphere) corresponding to a cooling tendency consistent with the vertical ascent needed to balance the lateral mass influx near the surface. We note $\nabla \cdot AHT$ diagnosed from Equation 2 is unaffected by any potential mass imbalance in ERA5 since adding a (vertical invariant) mass flux convergence to the column makes no impact on $\nabla \cdot AHT$ as

$$\int_0^{\overline{Ps}} MSE^{\dagger} = 0 \tag{3}$$

by definition. Thus, this definition of ∇ -AHT represents the contrast of energy entering and leaving a fixed mass of atmospheric column. Consistently, we define the atmospheric column energy tendency as:

Column tendency =
$$\int_{0}^{\overline{Ps}} \frac{d(c_p T + L_v Q)}{dt} dp$$
 (4)

which represents the change in the average energy content of a fixed mass atmospheric column and is diagnosed from the centered finite difference of 6 hourly ERA5 data. The moisture flux convergence is calculated from Equation 2 by replacing MSE with $L_{\nu}Q$. All quantities are (area weighted) averaged over a sector centered on Dome C of 50° longitude by 25° latitude (62.5–88.5°S and 98–148°E) and are low pass filtered using a 6-day cutoff period.

2.3. GCM Simulations

To assess how well a climate model may simulate such a heatwave, we use the fully coupled NCAR CESM1-CAM5 GCM and diagnose output from its 35-member large ensemble (CESM-LENS; Kay et al., 2015), which is

19448007, 2023, 17, Downloaded from https://agupubs.onlinelibrary.wiley.com/doi/10.1029/2023GL104910 by University Of Washington, Wiley Online Library on [19/10/2023]. See the Terms

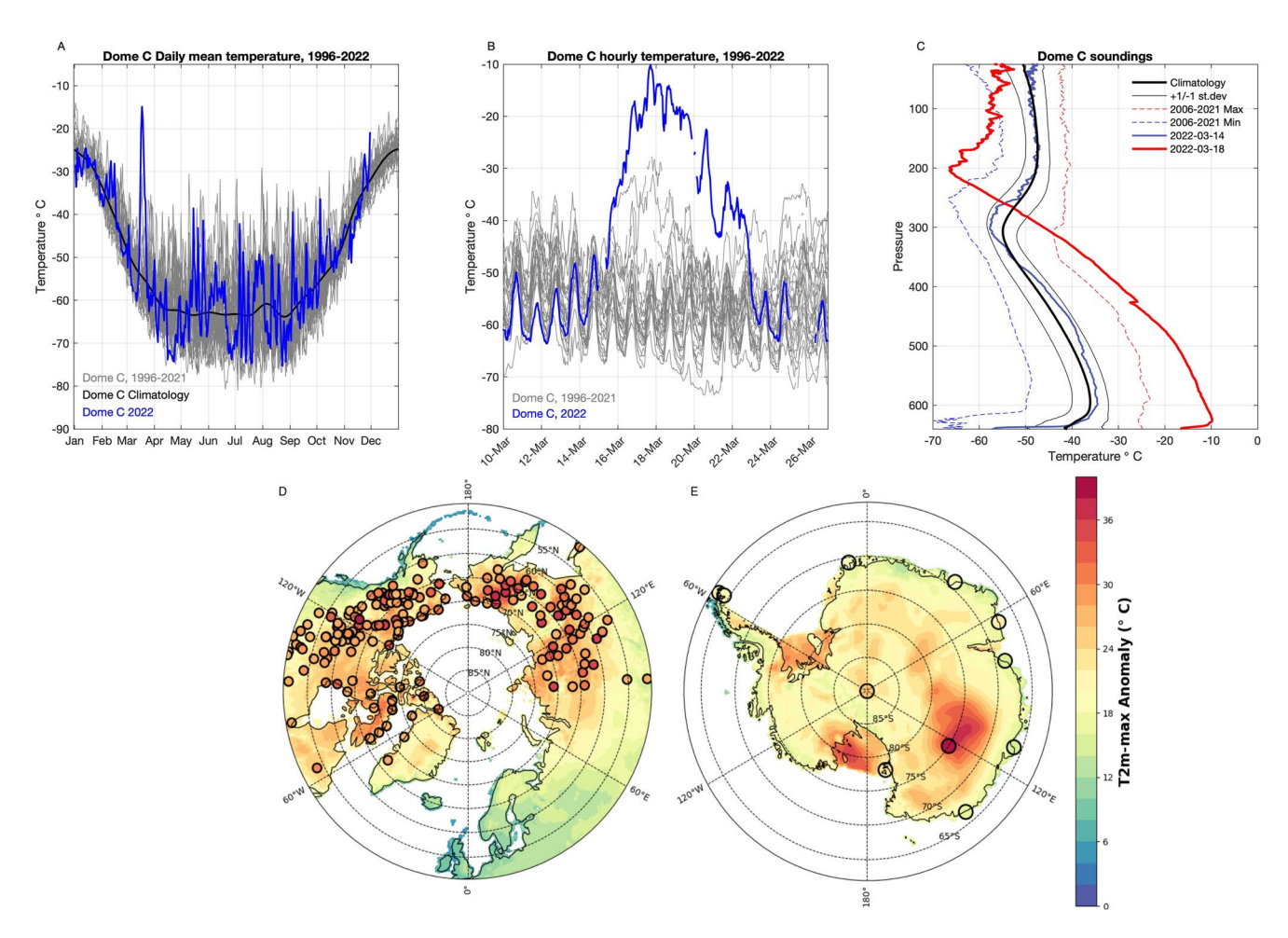


Figure 1. (a) Dome C daily temperatures over 1996–2021 (gray), 2022 (blue), and the climatology (black), (b) as in (a), but hourly temperature for mid-March (the *x*-axis are labeled at 12UTC on the dates shown), (c) Dome C radiosonde temperatures during and prior to the heatwave (red and blue), March climatology (black), and March extreme maximum and minimum values over 2006–2021 (red and blue dashed), and (d, e) largest recorded heatwaves globally, quantified with station data (shaded dots, only top-200 events shown for clarity), and ERA5 (background shading). Extreme heatwaves are all recorded poleward of 50°in both hemispheres, for clarity we do not show areas outside these regions.

forced with historical forcing over 1850–2005 and the high emission RCP8.5 scenario over 2006–2100. CESM1-CAM5 is among the CMIP5 models with highest fidelity compared to observations (Knutti et al., 2013). To assess the role of atmospheric circulation biases in CESM1-CAM5 on simulating a comparable heatwave, we have produced new simulations (referred to as CESM-Nudge2022) with CESM1-CAM5 in which meridional and zonal winds between the top of the model and 850 hPa are nudged toward ERA5 winds, following the methodology described in Blanchard-Wrigglesworth et al. (2021) and Supporting Information S1. To assess the role of climate change on the amplitude of the heatwave, we produce additional simulations that nudge to observed 2022 winds but under 1922 and 2096 climate forcing (referred to as CESM-Nudge1922 and CESM-Nudge2096) that quantify the (thermodynamic) past and future contribution of anthropogenic-forced climate change respectively. To assess the influence of Southern Ocean SST March 2022 anomalies on the heatwave, we produce an additional simulation equivalent to CESM-Nudge2022 that also nudges SSTs over the Southern Ocean north of the sea ice (40°S–56°S) to the 1980–2010 model climatology (referred to as CESM-Nudge2022_climoSST).

3. Results

3.1. The March 2022 Heatwave

Daily mean temperatures at Dome C rose from near climatology (-54°C) on 15 March to -15°C on 18 March, before dropping back to climatology by 24 March (Figure 1). Hourly temperatures peaked at -10.1°C on 18

March, the highest recorded hourly temperature at Dome C over the station's lifetime (1996–2022, Figure S1a in Supporting Information S1), beating summer maxima when climatology is 30° C warmer and incoming top of atmosphere solar radiation is 4 times greater (\sim 530 W/m² in December compared to \sim 130 W/m² in mid-March). On 18 March, the daily mean temperature at Dome C was 39° C warmer than climatology and 16° C warmer than the previous March record (-31° C). Remarkably, the temperature remained above the previous March record for 3 consecutive days, including during the nighttime. In terms of year-round anomalies from climatology, this event amply beat the previous record (33° C) at Dome C, recorded in winter when variability is greater, and is a 6 standard deviation (σ) anomaly, 2σ greater than any other anomaly (Figures S1c and S1d in Supporting Information S1). We find that the heatwave set a new global record temperature anomaly, using both ERA5-reanalysis (38° C) and Dome C weather station data (39° C). Figures 1d and 1e shows spatial maps of the largest positive daily maximum temperature anomaly in both hemispheres. Only a handful of heatwaves have been observed with magnitudes greater than 35° C, all at high latitudes in Siberia, North America, and Antarctica. In terms of normalized anomalies, a 6σ anomaly is also the largest temperature extreme estimated globally (cf. Thompson et al. (2022)).

Temperatures below the 300 hPa level (\sim 8 km in height) were warmer than the previous March records (Figure 1c), with anomalies of 18–22°C (equivalent to 5σ) at 400 and 500 mb, and surface-amplified temperature anomalies as the climatological inversion layer weakened (Figure S2b in Supporting Information S1). The 18 March profile shows a peak temperature of -10° C atop the surface inversion layer, matching the highest surface temperature recorded a few hours earlier, suggesting that the highest surface hourly temperature recorded on 18 March resulted from the inversion layer being completely eroded during daylight hours prior to the radiosonde profile, as further evidenced by the Dome C tower 2 and 40 m temperatures (Figure S2d in Supporting Information S1). Relative humidity values increased from near climatology (40%–60%) on 14 March to 70%–95% throughout the troposphere on 18 March (Figure S3a in Supporting Information S1), though satellite imagery shows cloud cover being advected into EEA from the north over 15–18 March (Movie S1), implying saturated air above Dome C. Total column integrated water vapor at Dome C peaked on 18 March at over 4 kg/m², a record maximum for the whole calendar year over 1979–2022 at Dome C (Figure S3b in Supporting Information S1). During the heatwave the tropopause rose from \sim 300 to \sim 200 hPa and the stratosphere cooled to record low March values, registering temperature anomalies of -15° C, equivalent to a -6σ anomaly that is as extreme as the surface temperature normalized anomaly (Figure S2c in Supporting Information S1).

3.2. Synoptic Situation

In Figure 2 and Figure S4 in Supporting Information S1 we show daily mean surface (T2m) and 500 hPa (T500) temperature anomalies and heights (Z500) and Z500 anomalies during the heatwave in ERA5. Surface temperatures on 14 March were slightly below climatology over EEA and near climatology over the Southern Ocean north of EEA. On 14 March, a pronounced atmospheric trough is present at 100°E, with a ridge starting to develop downstream along 120°E, and 8-12°C T500 anomalies present on 14 March over the Southern Ocean north of EEA. Over the following 3 days, large T2m and T500 anomalies built over EEA, as an omega block pattern developed (Figure S4b in Supporting Information S1) and the ridge strengthened leading to near-record northerly winds over EEA (Figure S5 in Supporting Information S1). The T2m anomalies were larger than the T500 anomalies, consistent with the radiosonde observations of a surface amplification of tropospheric temperature anomalies. A back-trajectory analysis shows that the airmass over EEA on March 17 and March 18 originated over southeast Australia 4 days prior (Figure 2b). On 19 March the atmospheric ridge started to break down, and a more zonal flow returned to the Southern Ocean north of EEA by 20 March. Over EEA, the circulation on 19-21 March stagnated under an anticyclonic regime, with the anomalously warm airmass rotating anticyclonicly in place (Figure S5a in Supporting Information S1) and cooling toward climatology (Figure 1b). Total-column integrated water vapor anomalies (Movie S2) show advection of anomalously high moisture from SE Australia toward EEA over 15–17 March. Two additional moisture sources can be identified over the SE Indian Ocean on 13 March and over South Africa on 11 March, which advected eastward and became entrained into the main EEA-bound northerly circulation over 15-17 March, While Dome C does not record precipitation, ERA5 estimates show significant precipitation along the EEA coastline, with over 100 mm accumulated over 15–18 March (Figure S5 in Supporting Information S1).

3.3. Atmospheric Heat Fluxes

The evolution of the T2m and T500 anomalies and origin of the heatwave airmass suggest strong meridional winds and large-scale dynamics drove the heatwave. To further explore the heatwave's drivers, we inspect the

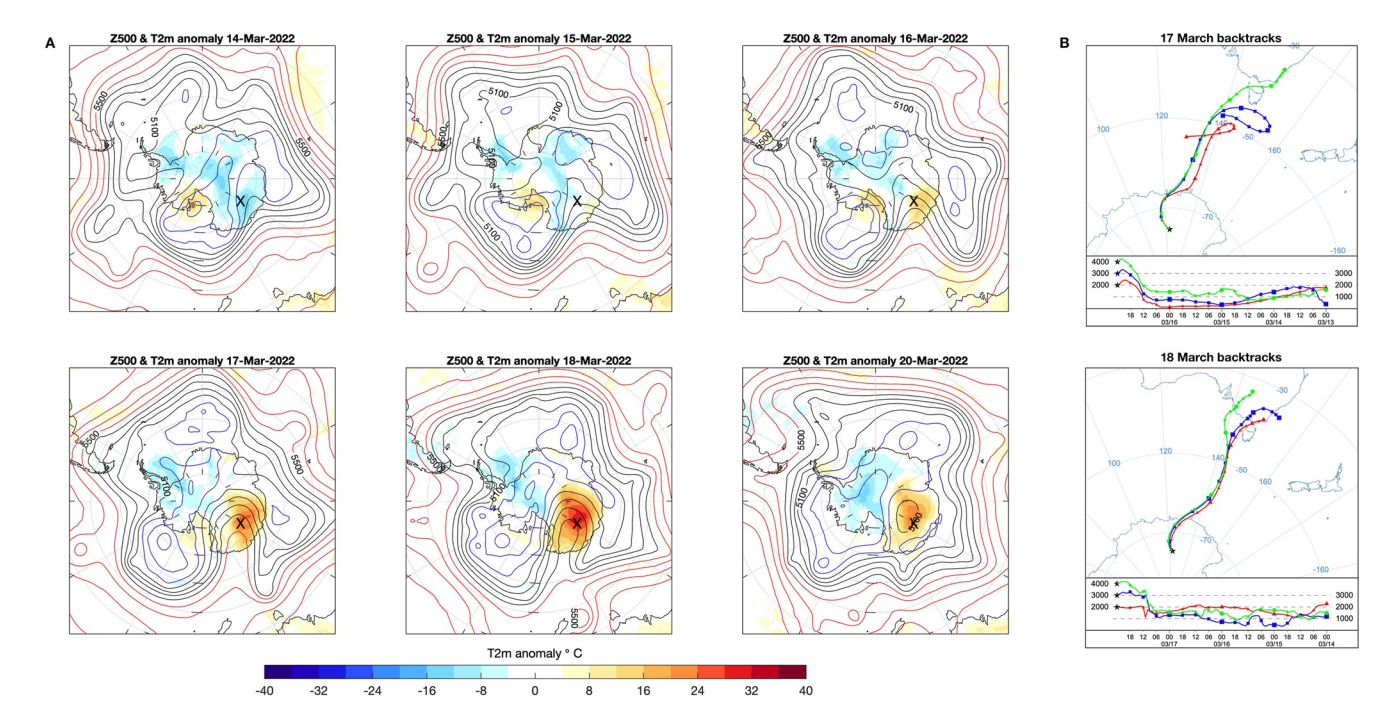


Figure 2. (a) Z500 and T2m anomalies from 14 March to 18 March, and 20 March. The black X marks the location of Dome C, and (b) 4-day back-trajectories from Dome C on 17 and 18 March, as calculated by the NOAA HYSPLIT model, from 3 different initialized elevations.

AHT convergence over EEA (Figure 3a). The AHT is highly correlated (R = 0.87) with the heating of the atmospheric column (Figure 3b) with a near 1:1 relationship suggesting that EEA heating and cooling events are initiated by atmospheric advection and are limited by the heat capacity of the atmospheric column, while radiative processes and surface energy exchange play a secondary role. In March 2022, a 5σ anomaly in AHT convergence (Figure 3a) in the 4 days preceding the heatwave provided enough energy to account for the heating of the atmospheric column. While this is the largest normalized anomaly, it is interesting to note that there are larger absolute magnitude AHT convergence events during the Austral winter, including one in June of 1992 that is also associated with larger magnitude atmospheric column heating (blue dots in Figure 3b). However, these other events are not associated with as much surface heating as the March 2022 heatwave because the atmospheric heating is spread throughout the atmospheric column (not shown) as opposed to the surface amplified warming with stratospheric cooling pattern of the March 2022 event (Figure 1c). What caused the AHT convergence induced warming to be surface amplified in the March 2022 event? One possible explanation is that moisture fluxes—which tend to be concentrated lower in the atmosphere—contributed disproportionately to the AHT convergence during this event (Figure 3c). In general, moisture fluxes contribute approximately 20% of the annual mean AHT convergence climatology and variability (cf. Figures 3a and 3c). However, during the March 2022 heatwave the moisture flux convergence (a 9σ anomaly) drove about 80% of the AHT convergence. In EEA, the moisture convergence is primarily precipitated and results in latent heating of the atmospheric column (Figure 3d).

3.4. Predictability of the Heatwave

How well did weather forecasts anticipate the heatwave? To answer this question, we assess forecast skill of the heatwave in the ECMWF high-resolution (9 km) operational 10-day deterministic forecasts from its IFS Cycle 47r3 model version. We focus on the ECMWF's forecast model as its forecasts have consistently the highest skill globally and for extreme events in polar regions (e.g., Blanchard-Wrigglesworth et al., 2022; Yamagami et al., 2018). ECMWF forecasts (Figure 4) were remarkable skilled at 8 days and shorter lead times, albeit with a surface cold bias of about $-5/-10^{\circ}$ C relative to observations. The temperature above the surface inversion layer was skillfully forecast, especially at 0–5 days leadtimes, as was the large scale circulation pattern characterized by the Z500 heights. The surface cold bias in the forecasts combined with the accurate prediction of free troposphere temperatures shows that forecasts struggled to predict the observed weakening of the surface inversion, a

19448007, 2023, 17, Downloaded from https://agupubs.onlinelibrary.wiley.com/doi/10.1029/2023GL104910 by University Of Washington, Wiley Online Library on [19/10/2023]. See the Terms and Condition

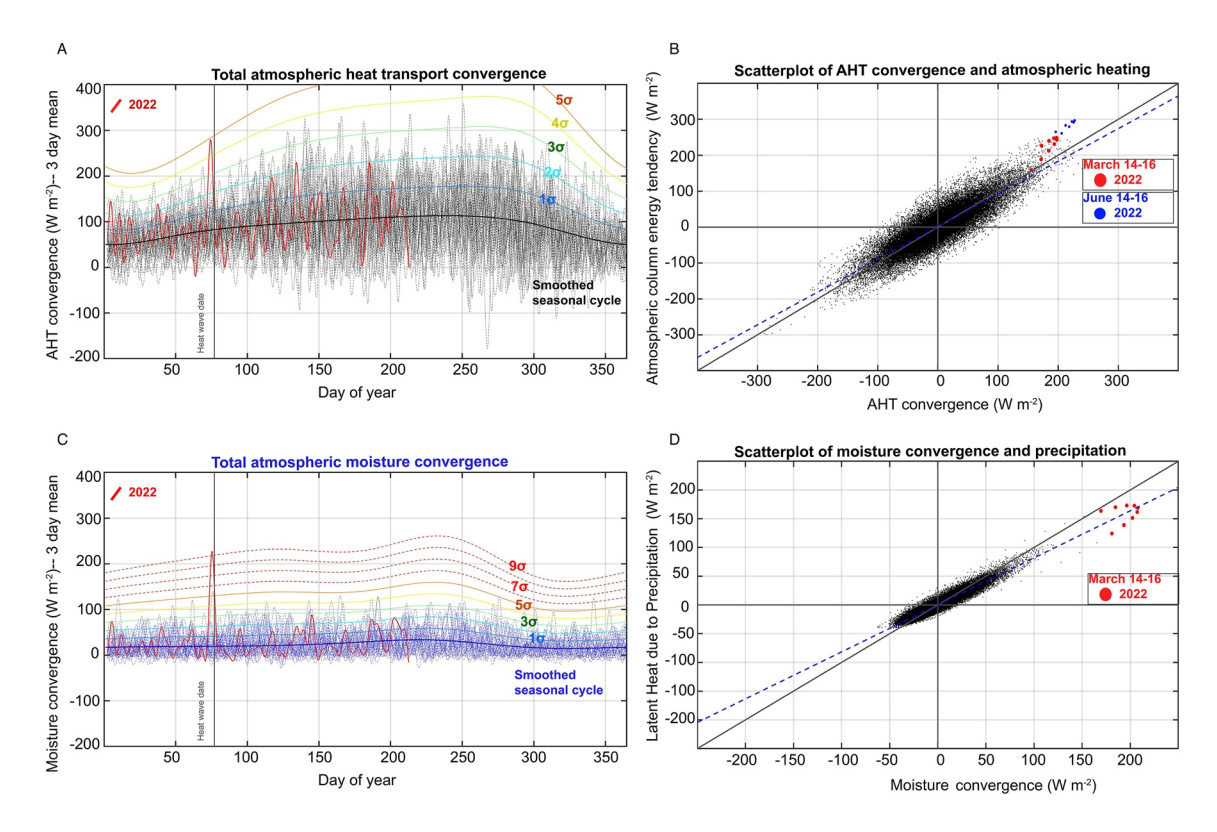


Figure 3. Dome C (a) atmospheric heat flux (AHT) convergence, (b) scatterplot of (deseasonalized) atmospheric column energy tendency versus AHT convergence, (c) atmospheric moisture flux convergence, and (d) scatterplot of (deseasonalized) latent heat due to precipitation versus atmospheric moisture flux convergence in ERA5 over 1979–2022. Values for 2022 are shown by the bold lines in the time series and values for the 2 days preceding the March 2022 heatwave are shown by red dots in the scatter plots. Smoothed seasonal cycle and standard deviation departures from averages are shown by the colored labeled lines. All quantities are low pass filtered using a cutoff period of 6 days and expressed in W/m².

feature that interestingly is also present in ERA5, which shows a surface temperature bias of about -5° C relative to observations (Figure 4a) but an accurate reproduction of 500 mb temperatures during the heatwave (Figure 4b).

3.5. Can a GCM Capture Such a Heatwave?

Daily mean temperatures at Dome C in CESM-LENS show that the model does not simulate a heatwave of comparable magnitude to observations (Figure 5a). The largest March heatwave that CESM-LENS simulates peaks at -27°C, 25°C warmer than the model climatology, an anomaly that is 14°C smaller than the observed March 2022 anomaly. Is the inability of the model to simulate such an event due to the heatwave resulting from an anomalous atmospheric circulation pattern beyond the model's internal variability, in which case, the model may simulate the observed heatwave with the "right" atmospheric circulation? Or is it due to model shortcomings in simulating other processes such as radiation, cloud microphysics/phase, boundary layer physics, or resolution?

To address this we analyze CESM-Nudge2022. This simulation better captures the March 2022 heatwave (Figure 5a), with Dome-C daily mean temperatures peaking at -20°C and surpassing the mid-March CESM-LENS record by up to 7°C (Figure 5b). While the nudged simulations show a surface temperature bias of about -5/-10°C with respect to station observations, this is a similar bias as that in ERA5 reanalysis and the ECMWF forecasts (Figure 4), arguably fairer comparison products for a GCM than station-based point observations.

3.6. The Impact of Climate Change

Traditionally, the role of climate change on heatwaves has been assessed via a statistical approach that quantifies the impact of climate change on the change in frequency of an event (e.g., Stott et al., 2016). However, determining even present return periods can be highly uncertain. For example, current return period estimates for the Pacific Northwest heatwave of June 2021 range from a 1 in 200 years event (Bartusek et al., 2022) to a 1 in

19448007, 2023, 17, Downloaded from https://agupubs.onlinelibrary.wiley.com/doi/10.1029/2023GL104910 by University Of Washington, Wiley Online Library on [19/10/2023]. See the Terms and Conditions (https://onlinelibrary.wiley

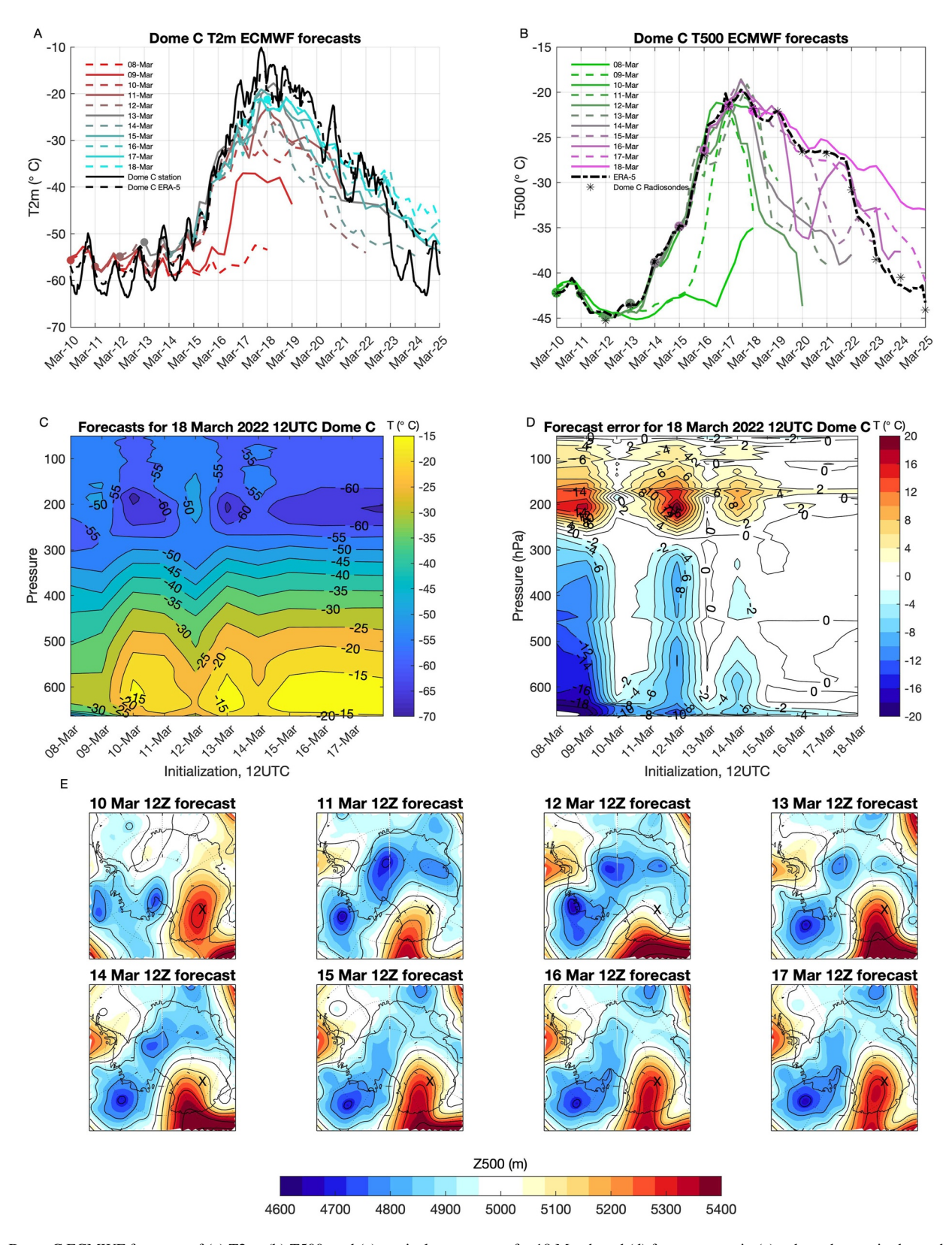


Figure 4. Dome C ECMWF forecasts of (a) T2m, (b) T500, and (c) vertical temperature for 18 March and (d) forecast error in (c), where the *x*-axis shows the initialization date for the 12 UTC forecasts, and (e) forecasts of Z500 targeting 18 March 2022, initialized from 10 March 2022 to 17 March 2022.

19448007, 2023, 17, Downloaded from https://agupubs.onlinelibrary.wiley.com/doi/10.1029/2023GL104910 by University Of Washington, Wiley Online Library on [1910/2023]. See the Terms and Conditions (https://onlinelibrary.wiley.com/terms

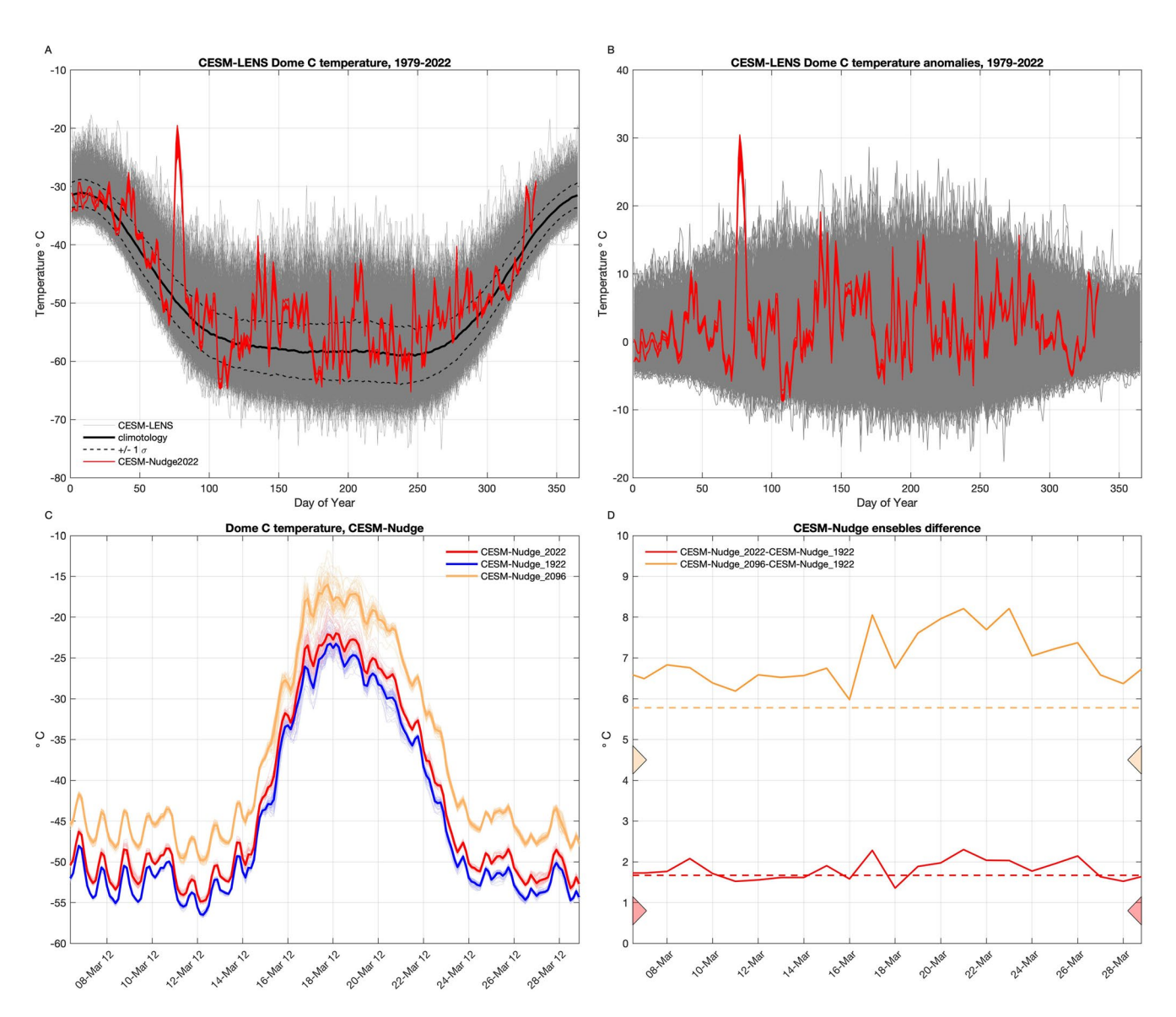


Figure 5. (a) Dome C daily temperatures over 1979–2022 for all 35 ensemble members of CESM-LENS (gray), the 1979–2022 climatology (black) and $+1/-1\sigma$ (dashed black), and CESM-Nudge2022 (red), (b) as in (a), but showing daily mean temperature anomalies with respect to the CESM-LENS climatology, (c) Dome C 3-hourly temperatures in CESM-Nudge2022 (red), CESM-Nudge1922 (blue), and CESM-Nudge2096 (orange), (d) ensemble-mean differences between CESM-Nudge2022 and CESM-Nudge1922 (red), and CESM-Nudge1922 (orange). The dashed lines in (d) show the CESM-LENS ensemble-mean temperature change at Dome C for March between 2022 and 1922 (red) and 2096 and 1922 (orange), the triangles show the mean global temperature change between the same periods.

10,000–100,000 years event (McKinnon & Simpson, 2022). An alternative methodology is to use the "storyline" approach (Sánchez-Benítez et al., 2022; Shepherd et al., 2018), in which observed heatwaves are reproduced in climate models by nudging the model's circulation to observations. The thermodynamic impact of climate change can then be assessed by nudging the model to the same circulation but under different forcing scenarios, as we do in CESM-Nudge1922 and CESM-Nudge2096 (Figure 5c). As expected, the CESM-Nuge1922 (CESM-Nudge2096) simulations are colder (warmer) than CESM-Nudge2022. The difference between the simulations (Figure 5d) shows that CESM-Nudge2022 is about 2°C warmer than the CESM-Nudge1922, which is slightly warmer than the local March climate change simulated by CESM-LENS (1.8°C), and significantly warmer than the mean warming in CESM-LENS between 2022 and 1922 (0.8°C). In CESM-Nudge2096, the simulated heatwave is 8°C warmer than in CESM-Nudge1922. By 2096, the local March climate change in CESM-LENS is 6°C, whereas the global climate change between 1922 and 2096 in CESM-LENS is 4.5°C. Thus the heatwave's amplitude is magnified by at least the local forced climate change, and there is evidence that the heatwave is further amplified,

warming of 8°C between 20 March and 24 March in Figure 5d).

3.7. Did the Record Minimum Sea Ice Matter?

The heatwave immediately followed the record minimum Antarctic sea ice extent of February 2022 (e.g., Turner et al., 2022a, 2022b). Since sea ice extent anomalies tend to also be anticorrelated with SST anomalies (Blanchard-Wrigglesworth et al., 2011, 2021), it is natural to ask if anomalous Southern Ocean SIC and SSTs played a role in amplifying the heatwave. To answer this question, we have run an additional ensemble that nudges the SSTs over the Southern Ocean to the 1980-2010 climatology (in addition to nudging the winds to observations). In this experiment (CESM-Nudge2022_climoSST), the magnitude of the heatwave is reduced by just 0.5–1°C relative to CESM-Nudge2022 (Figure S6 in Supporting Information S1). The small impact is likely due to March 2022 SSTs being 1-2°C warmer than average around SE Australia (the source region of the heatwave airmass, and which are skillfully reproduced in CESM-Nudge2022), but close to climatology north of EEA (Figure S6 in Supporting Information S1) along the path of the airmass (Figure 2b).

4. Discussion

The March 2022 Antarctic heatwave was a historic event, registering temperature anomalies of 39°C above climatology that rank it as the largest recorded heatwave. The heatwave resulted from a highly anomalous atmospheric circulation pattern that caused extreme northerly winds and AHT convergence, as an airmass of Australian origin advected into the interior of EEA over just 4 days. Associated moisture heat fluxes played a key role in driving the heating over the EEA and in producing surface-amplified temperature anomalies. The event was well forecast by the ECMWF model at 8-day and shorter lead times, even if the model under-forecasts the surface amplitude of the heatwave by 5-10°C. A widely used GCM, NCAR's CESM1-CAM5, does not simulate comparable EEA heatwaves in a large ensemble simulation, and the largest Dome C anomaly it can simulate is 25°C. However, once the model's circulation is nudged toward observations, the model can simulate a 31°C anomaly heatwave (or about 80% of the observed heatwave), suggesting model biases in simulating blocking events over EEA (Patterson et al., 2019) are a key source of error in simulating extreme EEA heatwaves and providing a roadmap for future model development to improve the simulation of extreme heatwaves. While the nudged simulations still under-estimate the surface temperatures during the heatwave by 5/10°C, this is a similar bias to that in ERA5 and ECMWF forecasts and may suggest a common bias among these models in simulating the observed warming. By also nudging the model's Southern Ocean SSTs to climatology, we find that the preceding February 2022 record minimum Antarctic sea ice cover did not significantly impact the heatwave, likely due to SSTs north of the EEA being close to climatology during March 2022. Using a "storyline" approach, we find that climate change over the last century amplified the heatwave by 2°C, while an equivalent heatwave in 2096 would be a further 6°C warmer relative to 2022 (8°C relative to 1922), raising the prospect of near-freezing temperatures over the EEA icecap during extreme late 21st century heatwaves under a high emissions scenario. These levels of warming are more than double the amount of global warming in the model over the same periods (0.8°C warming and 4.5°C warming over 1922–2022 and 1922–2096 respectively) and slightly warmer than the local March forced warming (1.8°C warming and 6°C warming over 1922-2022 and 1922-2096 respectively), suggesting an amplification of the magnitude of the heatwave beyond the local warming expected from forced climate change as found for mid-latitude heatwaves (Bartusek et al., 2022; Sánchez-Benítez et al., 2022; Wehrli et al., 2020).

Data Availability Statement

ERA5 data (Hersbach et al., 2020) are available at https://www.ecmwf.int/en/forecasts/dataset/ecmwf-reanalysis-v5, Dome C station data are available at https://amrc.ssec.wisc.edu/, the radiosonde data are available at https://www.climantartide.it/dataonline/rds/index.php?lang=en, and Dome C tower 2 and 40 m temperature observations are available at https://web.lmd.jussieu.fr/~cgenthon/SiteCALVA/Datas/temp22+.dat. Global temperature station data are available at https://www.ncei.noaa.gov/products/land-based-station/global-historical-climatology-network-daily. ECMWF forecast data are available at https://www.ecmwf.int/en/forecasts/ dataset/operational-archive, copyright 2022 European Centre for Medium-Range Weather Forecasts (ECMWF). CESM-LENS data are available via https://www.cesm.ucar.edu/community-projects/lens/data-sets. Output from the nudged simulations is available at https://atmos.washington.edu/~ed/data/. NSIDC sea ice concentration area available at https://doi.org/10.7265/efmz-2t65 and NOAA ERSSTv5 SST data area available at https://psl.noaa.gov/data/gridded/data.noaa.ersst.v5.html.

Acknowledgments

EBW and AD acknowledge the generous support of the National Science Foundation Office of Polar Programs through award 2233016. TC acknowledged the generous support of the National Science Foundation Award CLD2019647. ZE is supported by the U.S. Department of Energy, Office of Science, Office of Advanced Scientific Computing Research, Department of Energy Computational Science Graduate Fellowship under Award Number(s) DE-SC0023112. We also thank Etienne Vignon and Christophe Genthon for help with Dome C data access and Dargan Frierson, Thomas Bracegirdle, Brian Rose, and Ian Eisenman for helpful discussions. This work uses ERA5 data, which contains modified Copernicus Climate Change Service information 2020. Neither the European Commission nor ECMWF is responsible for any use that may be made of the Copernicus information or data it contains. We acknowledge the NOAA Air Resources Laboratory (ARL) for the provision of the HYSPLIT transport and dispersion model and/or READY website (https://www.ready.noaa.gov) used in this publication. We would also like to acknowledge high-performance computing support from Cheyenne (https://doi. org/10.5065/D6RX99HX) provided by NCAR's Computational and Information Systems Laboratory, sponsored by the National Science Foundation.

References

- Bartusek, S., Kornhuber, K., & Ting, M. (2022). 2021 North American heatwave amplified by climate change-driven nonlinear interactions. Nature Climate Change, 12(12), 1–8. https://doi.org/10.1038/s41558-022-01520-4
- Blanchard-Wrigglesworth, E., Armour, K., Bitz, C. M., & de Weaver, E. (2011). Persistence and inherent predictability of Arctic sea ice in a GCM ensemble and observations. *Journal of Climate*, 24(1), 231–250. https://doi.org/10.1175/2010JCLI3775.1
- Blanchard-Wrigglesworth, E., Roach, L. A., Donohoe, A., & Ding, Q. (2021). Impact of winds and Southern Ocean SSTs on Antarctic sea ice trends and variability. *Journal of Climate*, 34(3), 949–965. https://doi.org/10.1175/jcli-d-20-0386.1
- Blanchard-Wrigglesworth, E., Webster, M., Boisvert, L., Parker, C., & Horvat, C. (2022). Record Arctic cyclone of January 2022: Characteristics, impacts, and predictability. *Journal of Geophysical Research: Atmospheres*, 127(21), e2022JD037161. https://doi.org/10.1029/2022jd037161
 DeConto, R. M., & Pollard, D. (2016). Contribution of Antarctica to past and future sea-level rise. *Nature*, 531(7596), 591–597. https://doi.org/10.1038/nature17145
- Dobricic, S., Russo, S., Pozzoli, L., Wilson, J., & Vignati, E. (2020). Increasing occurrence of heat waves in the terrestrial Arctic. *Environmental Research Letters*, 15(2), 024022. https://doi.org/10.1088/1748-9326/ab6398
- Donohoe, A., & Battisti, D. S. (2013). The seasonal cycle of atmospheric heating and temperature. *Journal of Climate*, 26(14), 4962–4980. https://doi.org/10.1175/jcli-d-12-00713.1
- England, M. R., Polvani, L. M., Sun, L., & Deser, C. (2020). Tropical climate responses to projected Arctic and Antarctic sea-ice loss. *Nature Geoscience*, 13(4), 275–281. https://doi.org/10.1038/s41561-020-0546-9
- González-Herrero, S., Barriopedro, D., Trigo, R. M., López-Bustins, J. A., & Oliva, M. (2022). Climate warming amplified the 2020 record-breaking heatwave in the Antarctic Peninsula. Communications Earth & Environment, 3(1), 122. https://doi.org/10.1038/s43247-022-00450-5
- Hersbach, H., Bell, B., Berrisford, P., Hirahara, S., Horányi, A., Muñoz-Sabater, J., et al. (2020). The ERA5 global reanalysis. *Quarterly Journal*
- of the Royal Meteorological Society, 146(730), 1999–2049. https://doi.org/10.1002/qj.3803

 Huang, B., Thorne, P. W., Banzon, V. F., Boyer, T., Chepurin, G., Lawrimore, J. H., et al. (2017). Extended reconstructed sea surface temperature version 5. (FRSCTVS). Uneraded validations and intercomparisons. Journal of Climate, 20(20), 2170, 2305. https://doi.org/10.1175/
- ature, version 5 (ERSSTv5): Upgrades, validations, and intercomparisons. *Journal of Climate*, 30(20), 8179–8205. https://doi.org/10.1175/jcli-d-16-0836.1

 Kay, J., Deser, C., Phillips, A., Mai, A., Hannay, C., Strand, G., et al. (2015). The Community Earth System Model (CESM) large ensemble
- project: A community resource for studying climate change in the presence of internal climate variability. *Bulletin of the American Meteorological Society*, 96(8), 1333–1349. https://doi.org/10.1175/bams-d-13-00255.1
- Knutti, R., Masson, D., & Gettelman, A. (2013). Climate model genealogy: Generation CMIP5 and how we got there. *Geophysical Research Letters*, 40(6), 1194–1199. https://doi.org/10.1002/grl.50256
- Konovalov, I., Beekmann, M., Kuznetsova, I. N., Yurova, A., & Zvyagintsev, A. (2011). Atmospheric impacts of the 2010 Russian wildfires: Integrating modelling and measurements of an extreme air pollution episode in the Moscow region. Atmospheric Chemistry and Physics, 11(19), 10031–10056. https://doi.org/10.5194/acp-11-10031-2011
- Lesk, C., Rowhani, P., & Ramankutty, N. (2016). Influence of extreme weather disasters on global crop production. *Nature*, 529(7584), 84–87. https://doi.org/10.1038/nature16467
- McKinnon, K. A., & Simpson, I. R. (2022). How unexpected was the 2021 Pacific Northwest heatwave? Geophysical Research Letters, 49(18), e2022GL100380. https://doi.org/10.1029/2022gl100380
- Meier, W. N., Fetterer, F., Windnagel, A. K., & Stewart, J. S. (2021). NOAA/NSIDC climate data record of passive microwave sea ice concentration, version 4. National Snow and Ice Data Center. https://doi.org/10.7265/efmz-2t65
- Patterson, M., Bracegirdle, T., & Woollings, T. (2019). Southern hemisphere atmospheric blocking in CMIP5 and future changes in the Australia-New Zealand sector. *Geophysical Research Letters*, 46(15), 9281–9290. https://doi.org/10.1029/2019gl083264
- Perkins-Kirkpatrick, S., & Lewis, S. (2020). Increasing trends in regional heatwaves. *Nature Communications*, 11(1), 3357. https://doi.org/10.1038/s41467-020-16970-7
- Robinson, S. A., Klekociuk, A. R., King, D. H., Pizarro Rojas, M., Zúñiga, G. E., & Bergstrom, D. M. (2020). The 2019/2020 summer of Antarctic heatwaves. *Global Change Biology*, 26(6), 3178–3180. https://doi.org/10.1111/gcb.15083
- Sánchez-Benítez, A., Goessling, H., Pithan, F., Semmler, T., & Jung, T. (2022). The July 2019 European heat wave in a warmer climate: Storyline scenarios with a coupled model using spectral nudging. *Journal of Climate*, 35(8), 2373–2390. https://doi.org/10.1175/jcli-d-21-0573.1
- Shepherd, T. G., Boyd, E., Calel, R. A., Chapman, S. C., Dessai, S., Dima-West, I. M., et al. (2018). Storylines: An alternative approach to representing uncertainty in physical aspects of climate change. Climatic Change, 151(3–4), 555–571. https://doi.org/10.1007/s10584-018-2317-9
- Stein, A., Draxler, R. R., Rolph, G. D., Stunder, B. J., Cohen, M., & Ngan, F. (2015). NOAA's HYSPLIT atmospheric transport and dispersion modeling system. *Bulletin of the American Meteorological Society*, 96(12), 2059–2077. https://doi.org/10.1175/bams-d-14-00110.1
- Stott, P. A., Christidis, N., Otto, F. E., Sun, Y., Vanderlinden, J.-P., van Oldenborgh, G. J., et al. (2016). Attribution of extreme weather and climate-related events. Wiley Interdisciplinary Reviews: Climate Change, 7(1), 23–41. https://doi.org/10.1002/wcc.380
- Sutanto, S. J., Vitolo, C., Di Napoli, C., D?Andrea, M., & Van Lanen, H. A. (2020). Heatwaves, droughts, and fires: Exploring compound and cascading dry hazards at the pan-European scale. *Environment International*, 134, 105276. https://doi.org/10.1016/j.envint.2019.105276
- Tedesco, M., & Fettweis, X. (2020). Unprecedented atmospheric conditions (1948–2019) drive the 2019 exceptional melting season over the Greenland ice sheet. *The Cryosphere*, 14(4), 1209–1223. https://doi.org/10.5194/tc-14-1209-2020
- Thompson, V., Kennedy-Asser, A. T., Vosper, E., Lo, Y. E., Huntingford, C., Andrews, O., et al. (2022). The 2021 western North America heat wave among the most extreme events ever recorded globally. *Science Advances*, 8(18), eabm6860. https://doi.org/10.1126/sciadv.abm6860
- Trusel, L. D., Frey, K. E., Das, S. B., Karnauskas, K. B., Kuipers Munneke, P., Van Meijgaard, E., & Van Den Broeke, M. R. (2015). Divergent trajectories of Antarctic surface melt under two twenty-first-century climate scenarios. *Nature Geoscience*, 8(12), 927–932. https://doi.org/10.1038/ngeo2563
- Turner, J., Holmes, C., Caton Harrison, T., Phillips, T., Jena, B., Reeves-Francois, T., et al. (2022a). Record low Antarctic sea ice cover in February 2022. Geophysical Research Letters, 49(12), e2022GL098904. https://doi.org/10.1029/2022gl098904
- Turner, J., Lu, H., King, J. C., Carpentier, S., Lazzara, M., Phillips, T., & Wille, J. (2022b). An extreme high temperature event in coastal East Antarctica associated with an atmospheric river and record summer downslope winds. *Geophysical Research Letters*, 49(4), e2021GL097108. https://doi.org/10.1029/2021gl097108



Geophysical Research Letters

- 10.1029/2023GL104910
- Wang, S., Ding, M., Liu, G., Zhao, S., Zhang, W., Li, X., et al. (2022). New record of explosive warmings in East Antarctica. *Science Bulletin*, \$2095–\$9273.
- Wehrli, K., Hauser, M., & Seneviratne, S. I. (2020). Storylines of the 2018 Northern Hemisphere heatwave at pre-industrial and higher global warming levels. *Earth System Dynamics*, 11(4), 855–873. https://doi.org/10.5194/esd-11-855-2020
- White, R. H., Anderson, S., Booth, J. F., Braich, G., Draeger, C., Fei, C., et al. (2023). The unprecedented Pacific Northwest heatwave of June 2021. *Nature Communications*, 14(1), 727. https://doi.org/10.1038/s41467-023-36289-3
- Yamagami, A., Matsueda, M., & Tanaka, H. L. (2018). Medium-range forecast skill for extraordinary Arctic cyclones in summer of 2008–2016. Geophysical Research Letters, 45(9), 4429–4437. https://doi.org/10.1029/2018gl077278